Basal power reconstruction during cycling using a robust discrete-time PI observer

Maxime Chorin, John Jairo Martinez Molina, Samuel Vergès

Basal power reconstruction during cycling using a robust discrete-time PI observer

Chorin M. * **Martinez J.** ** **Vergès S.** ***

* *Univ. Grenoble Alpes, CNRS, Grenoble INP, GIPSA-lab, 38000 Grenoble, France (e-mail: maxime.chorin@grenoble-inp.fr).*
** *Univ. Grenoble Alpes, CNRS, Grenoble INP, GIPSA-lab, 38000 Grenoble, France (e-mail: john-jairo.martinez-molina@grenoble-inp.fr)*
*** *Univ. Grenoble Alpes, Inserm, CHU Grenoble Alpes, HP2, 38000 Grenoble, France (e-mail: SVerges@chu-grenoble.fr)*

Abstract: The basal metabolic rate characterizes the energy consumption of the human body at rest. It can be estimated by using respiratory gas exchange analyzers and indirect calorimetry. During cycling this value could vary due to several adaptation processes such as an increase in breathing and blood circulation, controlling body temperature, among others. In this paper we propose to reconstruct the instantaneous value of this basal metabolic rate, referred here as basal power (measured in Watts), by using a robust discrete-time proportional integral (PI) observer. The observer design is based on a solution of linear matrix inequalities and uses an uncertain linear parameter varying model of the gas exchange dynamics. The proposed methodology allows the reconstruction of the basal power while making the respiratory gas exchange estimation robust to bounded uncertainties and disturbances. The PI observer has been validated in simulation.

Keywords: Robust observers, uncertain linear parametric varying systems, linear matrix inequalities, physiological models.

1. INTRODUCTION

The basal metabolic rate (BMR) is a physiological quantity characterizing the energy consumption of the human body at rest and can be expressed in Watts. It comprises the minimum functions the body requires such as breathing, regulating the body temperature or ensuring the brain activity. It has been shown that the BMR varies between individual based on parameters like age, gender and weight Harris and Benedict (1918); McMurray et al. (2014); Melzer et al. (2016); Henry (2005). Also, the BMR can vary for a given individual depending on temperature McConnell (1925), altitude Grover (1963) or training level Gilliat-Wimberly et al. (2001). The BMR is closely linked with respiratory gas exchange (RGE) of a breathing individual, more precisely the oxygen consumption and the carbon dioxide production. Methods exploiting this connection are known under the name of indirect-calorimetry. In order to develop control laws allowing the regulation of physiological variables such as the respiratory gas exchanges or the energy expenditure, the variability of the BMR has to be taken into account. Thus, in this paper, we propose to estimate its value in real-time.

During a physical activity, the human ventilatory system adapts with an increase in the oxygen consumption and carbon dioxide production. To sustain a physical activity, adenosine triphosphate (ATP) is hydrolyzed to produce physical work and carbon dioxide. ATP resynthesis can occur with oxygen consumption (*aerobic reaction*), or without (*anaerobic reaction*). The aerobic pathway is known to be efficient and sustainable for long periods of time, whereas the anaerobic pathway, used to face intense energy expenditure, lasts only for short periods of time. The anaerobic pathway implies an excess of carbon dioxide produced, which can be measured in the gas exchanged during effort. Thus, gas exchange can provide indirect information regarding physiological reactions happening within the body. In sport medicine, gas exchange is used as a proxy to study individual physical capacities in a non-invasive way.

Gas exchange dynamics is a dynamical system that can be modeled and identified by using experimental data. Several model structures have been proposed into the literature to describe the behavior of this dynamical system. For example, Su et al. Su et al. (2007) and Baig et al. Baig et al. (2012) proposed to describe the evolution of the oxygen uptake using a Hammerstein model, respectively during treadmill exercise, and running and rowing. A combination of machine learning and wearable devices is also a popular approach to estimate gas exchange in a non-invasive way as shown in Altini et al. (2016); Beltrame et al. (2017); Shandhi et al. (2020). In Rosero et al. (2018), a linear parameter varying (LPV) system is proposed to model gas exchange during cycling. This model offers the advantage to estimate both the oxygen uptake (O_2) and the carbon dioxide production (CO_2) and proposes a novel way to discriminate the aerobic and anaerobic contributions in CO_2 production during effort. The latter model will be used in this paper to estimate gas exchange dynamics. This model supposes a constant BMR, which is identified using experimental data, and does not account for its variability

over time, which can lead to significant steady state errors in the respiratory gas exchange variables.

In this paper we explore the use of a Proportional Integral (PI) observer for estimating both the respiratory gas exchange variables (the amounts of O_2 intake and CO_2 output). Several methods for designing PI observers have been proposed in the literature, some of them are known under the name of disturbance observer based control (DOBC), to estimate and compensate the influence of disturbances and uncertainties on a closed-loop system. For continuous-time linear and non-linear frameworks, an extensive review of these methods can be found in Chen et al. (2016) and a chronological overview in Sariyildiz et al. (2020). DOBC can be found under different forms, in Ohishi et al. (1987) the disturbance is reconstructed using a filter with appropriate bandwidth, in Han (2009) an extended state observer (ESO) is proposed, Johnson (2008, 1968) developed the idea of unknown input observers (UIO) and She et al. (2008, 2011) equivalent input disturbances (EID). Here, we propose a PI observer design method based on a modified version of the robust set-membership observer proposed in Martinez et al. (2018). The considered gas exchange dynamics is an uncertain linear system with a linear parameter varying matrix output matrix (describing sensor nature). The proposed approach has been tested and validated in simulation.

The paper is organized as follows. First, in Section 2, the respiratory gas exchange model and its connections with the basal metabolic rate are presented and discussed. Then, in Section 3, the problem of basal reconstruction is described. In Section 4, we propose a methodology to derive a robust discrete-time PI observer reconstructing the basal power and the respiratory gas exchange variables. The observer is simulated in Section 5 and compared to a robust observer without integral action. Finally, we conclude this work in Section 6.

Notations used are standard. The hat $\hat{\cdot}$ refers to an estimated quantity. In linear matrix inequalities, $\star$ terms can be inferred from diagonal symmetry. The notation $\cdot(k)$ refers to the value of a vector at time instant k. The superscript $\cdot^T$ refers to the transposition. The symbol $\succeq$ means positive semidefinite, $\preceq$ negative semidefinite. I_n is the identity matrix of order n. Matrices and vectors are bolded, scalars are not.

2. GAS EXCHANGE MODEL

To model the dynamics of gas exchange during cycling, the following discrete time Linear Parameter Varying system has been proposed in Rosero et al. (2018) :

$$\begin{cases} \mathbf{x}(k+1) = \mathbf{A}\mathbf{x}(k) + \mathbf{B}(u(k) + w_0) \\ \mathbf{y}(k) = \mathbf{C}(\rho(k))\mathbf{x}(k) \end{cases} \quad (1)$$

where $\mathbf{x}(k) \in \mathbb{R}^3$ is the state vector given by $\mathbf{x}(k) = [x_1, x_2, x_3]^T$ with $x_1 = mO_2$ the consumed mass of oxygen per unit of time (in g/min), $x_2 = mCO_2$ the aerobically produced mass of carbon dioxide per unit of time (in g/min) and $x_3 = \varepsilon CO_2$ stands for the anaerobically produced mass of carbon dioxide per unit of time or excess of CO_2 (in g/min). The input $u(k) \in \mathbb{R}$ stands for the mechanical power developed by the cyclist at the pedal level (in Watts).

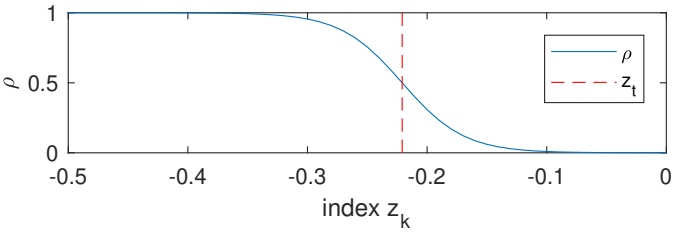

Fig. 1. Evolution of the transition function ρ along the index $z(k)$ in blue. The index corresponding to the anaerobic threshold (AT), z_T, is represented in red. The region right of z_T is considered mostly aerobic and the region left of z_T mostly anaerobic.

The symbol w_0 stands for an additional unknown power demand, the basal power (for instance, the power required for other physiological functions such as breathing, blood circulation, controlling body temperature, among others). Remark that in this model, the term w_0 inherits the units of watts observed from a pedal point of view.

The output vector $\mathbf{y}(k) \in \mathbb{R}^2$ is given by $\mathbf{y}(k) = [y_1, y_2]^T$ with $y_1 = x_1$ the consumed oxygen mass per unit of time (in g/min) and $y_2 = x_2 + \rho x_3$ the total carbon dioxide mass per unit of time (in g/min) mCO_2^{tot} formed by adding the aerobic CO_2 contribution to a fraction ρ of the excess of carbon dioxide εCO_2. Matrices $\mathbf{A}$ and $\mathbf{B}$ are constant. Matrix $\mathbf{C}(\rho(k))$ depends affinely in the parameter ρ as follows :

$$\mathbf{C}(\rho(k)) = \begin{pmatrix} 1 & 0 & 0 \\ 0 & 1 & \rho(k) \end{pmatrix} \quad (2)$$

Thus, system (1) is an LPV system with parameter dependent output.

Because the varying parameter $\rho(k)$, which is the fraction of excess of carbon dioxide present in the total mass of CO_2 measured in output of the system, is not a variable that can be directly measured in practice, it is modeled as the following function of the states :

$$\begin{cases} z(k) = x_1(k) - x_2(k) - \rho(k-1)x_3(k) \\ \rho(k) = 0.5 + 0.5\tanh\left(\frac{z_T - z(k)}{h}\right) \end{cases} \quad (3)$$

This model is inspired from the concept of anaerobic threshold, developed in physiology Wasserman (1984). During exercise, a physical effort is considered aerobic when the balance between the oxygen supply and the oxygen demand during the power production process is ensured, and considered anaerobic when it is not Spurway (1992). The shift between these two modes is called the anaerobic threshold and non-invasive determination methods through gas exchange have been proposed Beaver et al. (1986). By definition, ρ takes its values between 0 and 1, $\rho = 0$ corresponding to an aerobic effort and $\rho = 1$ corresponding to an anaerobic effort. The index $z(k)$ takes its values around 0 when there is a balance between mO_2 and mCO_2, corresponding to an aerobic effort. When the anaerobic threshold is crossed, the additional carbon

dioxide production due to εCO_2 implies a growth of $z(k)$ in the negatives values. z_T is the translation of the anaerobic threshold in the index $z(k)$ and h is scalar modulating the rate of variation between the aerobic and the anaerobic pathways. The transition function is represented in Fig.1.

This kind of models can be identified by using experimental data and by solving successive nonlinear least square problems as described in Rosero et al. (2018). An example of such a model for a given individual (that will be used here as the nominal model), is described by the following matrices and constants:

$$\mathbf{A} = \begin{pmatrix} 0.3398 & 0.5386 & 0 \\ 0 & 0.9303 & 0 \\ 0 & 0.1572 & 0.3458 \end{pmatrix}, \mathbf{B} = \begin{pmatrix} 0.0015 \\ 0.0015 \\ -0.0009 \end{pmatrix},$$

$$z_T = -0.2209, h = 0.0516, w_0 = 12.7621$$

for a sampling time $T_e = 3sec$.

3. PROBLEM STATEMENT

In practice, the model (1) undergoes disturbances on the state and the output due to unmodelled dynamics or measurement noise. In particular, the variability of w_0 has to be taken into account.

To do so, we propose the following disturbed version of model (1) :

$$\begin{cases} \mathbf{x}(k+1) = \mathbf{A}\mathbf{x}(k) + \mathbf{B}(u(k) + w_0 + p(k)) + \mathbf{F}d(k) \\ \mathbf{y}(k) = \mathbf{C}(\rho(k))\mathbf{x}(k) + \mathbf{Z}v(k) \end{cases} \tag{4}$$

where $p(k) \in \mathbb{R}$ is a piece-wise constant disturbance signal modelling unknown variations of the basal power with respect to the nominal one w_0, $d(k) \in \mathbb{R}$ and $v(k) \in \mathbb{R}$ are random signals representing respectively the state disturbance and the measurement noise. Matrix $\mathbf{F} \in \mathbb{R}^3$ and matrix $\mathbf{Z} \in \mathbb{R}^2$.

In order to recover the value of the unknown basal disturbance $p(k)$, we propose to use a proportional integral (PI) observer. To design such observer, we first extend the states of system (4) as follows :

$$\mathbf{x}_e(k) = \begin{bmatrix} \mathbf{x}(k) \\ p(k) \end{bmatrix} \tag{5}$$

We can now re-write (4) as :

$$\begin{cases} \mathbf{x}_e(k+1) = \mathbf{A}_e\mathbf{x}_e(k) + \mathbf{B}_e(u(k) + w_0) + \mathbf{F}_e d(k) \\ \mathbf{y}(k) = \mathbf{C}_e(\rho(k))\mathbf{x}_e(k) + \mathbf{Z}v(k) \end{cases} \tag{6}$$

with $\mathbf{A}_e = \begin{bmatrix} \mathbf{A} & \mathbf{B} \\ 0 & 1 \end{bmatrix}$, $\mathbf{B}_e = \begin{bmatrix} \mathbf{B} \\ 0 \end{bmatrix}$, $\mathbf{F}_e = \begin{bmatrix} \mathbf{F} \\ \theta \end{bmatrix}$ and $\mathbf{C}_e = [\,\mathbf{C}\ 0\,]$.

The coefficient $\theta > 0$, in matrix $\mathbf{F}_e$, is a constant parameter used during the observer design process. This coefficient is necessary to establish a non-zero transfer function between disturbances $d(k)$ and the extended state $p(k)$, allowing an H_∞ observer synthesis. The value of that parameter θ can be considered as a degree of freedom to design an observer with suitable speed convergence and noise attenuation.

Here, we assume that there exists a constant observer gain $\mathbf{L} \in \mathbb{R}^4$ such that the following parameter-dependent state observer can be performed for any value of $\rho(k)$ verifying (3):

$$\begin{cases} \hat{\mathbf{x}}_e(k+1) = \tilde{\mathbf{A}}_e(\rho(k))\hat{\mathbf{x}}_e(k) + \mathbf{B}_e(u(k) + w_0) + \mathbf{L}y(k) \\ \hat{\mathbf{y}}(k) = \mathbf{C}(\rho(k))\hat{\mathbf{x}}_e(k) \end{cases} \tag{7}$$

with $\tilde{\mathbf{A}}_e(\rho(k)) = \mathbf{A}_e - \mathbf{L}\mathbf{C}_e(\rho(k))$.

Now, defining the state estimation error at instant k as follows:

$$\mathbf{e}(k) = \mathbf{x}_e(k) - \hat{\mathbf{x}}_e(k) \tag{8}$$

we can write its dynamics as:

$$\mathbf{e}(k+1) = \tilde{\mathbf{A}}(\rho(k))\mathbf{e}(k) + \mathbf{E}\mathbf{w}(k) \tag{9}$$

with $\mathbf{E} = [\mathbf{F}\ -\mathbf{L}\mathbf{Z}]$ and $\mathbf{w}(k) = [d(k)\ v(k)]^T$.

Thus, the problem is to find a constant observer gain $\mathbf{L} \in \mathbb{R}^{n \times p}$ for the parameter dependent state-observer (7) such that for all $\boldsymbol{\rho}(k)$ the dynamics (9) are stable with a quadratic $\mathcal{H}_\infty$ performance γ, i.e. such that the ratio between the estimation error and the disturbance $\mathbf{w}(k)$ is bounded in the sense of the $\mathcal{L}_2$ norm: $\|\mathbf{e}(k)\|_2 < \gamma\|\mathbf{w}(k)\|_2$.

4. ROBUST PI OBSERVER DESIGN

The objective is to find a constant observer gain $\mathbf{L}$ ensuring the stability of the estimation error dynamics (9) and minimizing the influence of disturbances on the estimation error. This problem is easily solved for the case of linear time invariant (LTI) systems with a direct application of the Bounded Real Lemma (BRL) in which a linear matrix inequality (LMI) is solved in order to find the gain $\mathbf{L}$. However, for LPV systems like (1) using the previous method would imply to solve an infinite number of LMIs over the range of variation of $\boldsymbol{\rho}$, which is not tractable. To overcome this difficulty, an extension of the BRL to LPV systems was proposed in Apkarian et al. (1995). This extension is based on the assumption that the parameter dependent matrices involved in (1) are contained in a convex hull with known vertices, allowing to solve a finite number of LMIs for these vertices only. Based on this result, a method to design a robust set-membership observer for LPV systems was proposed by Martinez et al. (2018). This method is mainly focused on the case of constant output matrices $\mathbf{C}$ and $\mathbf{Z}$ in order to ease the translation of the problem in the form of LMIs, but an adaptation is proposed for the case of parameter dependent output matrices $\mathbf{C}$ and $\mathbf{Z}$.

Here, we propose an alternate solution to the observer design problem in the case of parameter varying matrix $\mathbf{C}_e(\rho)$ adapted from the work of Martinez et al. (2018).

Because $\rho(k) \in [0;1]$ for all k, and matrix $\mathbf{C}_e(\rho(k))$ depends affinely on $\rho(k)$, a polytopic decomposition can

be performed and matrix $\mathbf{C}_e(\rho(k))$ can be expressed as a linear combination of constant matrices as follows :

$$\mathbf{C}_e(\rho(k)) = \alpha_0(k)\mathbf{C}_{e0} + \alpha_1(k)\mathbf{C}_{e1} \tag{10}$$

where $\alpha_0 \geq 0$, $\alpha_1 \geq 0$ and for all k

$$\alpha_0(k) + \alpha_1(k) = 1 \tag{11}$$

Matrices $\mathbf{C}_{e0}$ and $\mathbf{C}_{e1}$ are the vertex matrices of the decomposition and are computed by evaluating $\mathbf{C}_e(\rho(k))$ its extreme values, respectively $\mathbf{C}_e(0)$ and $\mathbf{C}_e(1)$. In our case, coefficients $\alpha_0(k)$ and $\alpha_1(k)$ are not required for the implementation since the gain chosen for the state observer is constant (and not a linear combination of gains at the vertices).

We also operate such decomposition on the system matrices $\tilde{\mathbf{A}}_e(\rho(k))$:

$$\tilde{\mathbf{A}}_e(\rho(k)) = \alpha_0\tilde{\mathbf{A}}_{e0} + \alpha_1\tilde{\mathbf{A}}_{e1} \tag{12}$$

with $\tilde{\mathbf{A}}_{e0} = \mathbf{A}_e - \mathbf{L}\mathbf{C}_{e0}$ and $\tilde{\mathbf{A}}_{e1} = \mathbf{A}_e - \mathbf{L}\mathbf{C}_{e1}$. Now, we are ready to use the following theorem to derive a robust observer design method.

Proposition 1. System (9) is stable if there exist a symmetric positive definite matrix $\mathbf{P} \in \mathbb{R}^{n\times n}$, and a positive scalar $\gamma > 0$ such that, for j = {0,1},

$$\begin{pmatrix} -\mathbf{P}+\mathbf{Q} & 0 & \tilde{\mathbf{A}}_{ej}^T\mathbf{P} \\ 0 & -\gamma^2 & \mathbf{E}^T\mathbf{P} \\ \mathbf{P}\tilde{\mathbf{A}}_{ej} & \mathbf{P}\mathbf{E} & -\mathbf{P} \end{pmatrix} \preceq 0 \tag{13}$$

where $\mathbf{Q} \in \mathbb{R}^{4\times4}$ is a given (arbitrary) symmetric positive definite matrix. In addition, system (9), with output $\mathbf{z}(k) \coloneqq \mathbf{Q}^{1/2}\mathbf{e}(k)$ and input $\mathbf{w}(k)$, has a Quadratic H_∞ performance equal to γ. □

Now, the following result can be used to design a the robust observer :

Theorem 2. Consider the system (9) and a given symmetric matrix $\mathbf{Q} \succ 0$. The H_∞ norm of the system is less than $\gamma > 0$ if there exist symmetric positive definite matrices $\mathbf{P}$ and matrix $\mathbf{U}$ satisfying the following condition:

$$\begin{pmatrix} -\mathbf{P}+\mathbf{Q} & 0 & \mathbf{A}_{ej}^T\mathbf{P} - \mathbf{C}_{ej}^T\mathbf{U}^T \\ \star & -\gamma^2 & [\mathbf{P}\mathbf{F} \ -\mathbf{U}\mathbf{Z}]^T \\ \star & \star & -\mathbf{P} \end{pmatrix} \preceq 0 \tag{14}$$

for every vertex of the polytopic decomposition, j = {0,1}. □

Proof.

By replacing $\tilde{\mathbf{A}}_{ej}$ by its definition, the LMI (13) can be rewritten as :

$$\begin{pmatrix} -\mathbf{P}+\mathbf{Q} & 0 & {\mathbf{A}_{ej}}^T\mathbf{P} - {\mathbf{C}_{ej}}^T\mathbf{L}^T\mathbf{P} \\ \star & -\gamma^2 & [\mathbf{F} \ -\mathbf{L}\mathbf{Z}]^T\mathbf{P} \\ \star & \star & -\mathbf{P} \end{pmatrix} \preceq 0 \tag{15}$$

The inequality (15) is not linear because of the variable product $\mathbf{L}^T\mathbf{P}$ and is then not solvable. To make up for this, we use a change of variable by introducing the matrix $\mathbf{U} = \mathbf{P}\mathbf{L}$. This completes the proof.

The set of LMIs (14) can be solved easily using any convex programming solver and the robust observer gain computed as

$$\mathbf{L} = \mathbf{P}^{-1}\mathbf{U} \tag{16}$$

In this paper, the problem (14) is solved using CVX toolbox, a package for specifying and solving convex programs Grant and Boyd (2014), Grant and Boyd (2008).

5. RESULTS & DISCUSSION

To validate the observer design methodology described in Section 4, we compute a state observer for system (6) undergoing state and output disturbances (d and v), as well as a constant disturbance p on w_0.

We suppose that the model mismatch can be split into two contributions. First, a constant disturbance p, modelling a low bandwidth component due to the uncertainty on the value of w_0 and taking up to 100% of the hypothesized value for w_0. Then, a random component d following a uniform distribution, modelling a high bandwidth component and taking up to 10% of the hypothesized value for w_0.

We run a simulation under which the ideal system (1) is affected by the exact same disturbances and uncertainties as the ones chosen for the design. Finally, we assess the performances of the observer.

The measured output $y^m(k)$ is the total carbon dioxide production, mCO_2^{tot}. Thus :

$$\mathbf{C}(\rho(k)) = [0 \ 1 \ \rho(k)] \tag{17}$$

and

$$y^m(k) = \mathbf{C}(\rho(k))\mathbf{x}(k) + \mathbf{Z}v(k) \tag{18}$$

Assuming a measurement of mCO_2^{tot} is relevant because, in practice, mCO_2^{tot} is directly proportional to the volume of gas exhaled which is an easy quantity to measure using an oral pneumotachograph.

To simulate the behavior of the system, the scheduling parameter $\rho(k)$ is computed at each sample time using (3) and the states of system (4).

The output estimation is performed by computing $\hat{\rho}(k)$, an estimated value of $\rho(k)$ using (3) and the estimated states of (7).

We also suppose that the accuracy of the sensor used to measure $y^m(k)$ is $0.1g/min$.

In this example, we choose :

$\mathbf{F} = 0.1\mathbf{B}w_0$
$\mathbf{Z} = 0.1$
$\underline{\rho} = 0$
$\bar{\rho} = 1$
$d = 1$
$\bar{v} = 1$
$\theta = 0.25$

The system is affected by the following input and output disturbances :

$$\mathcal{D}_u = 0.1\mathbf{B}w_0 d$$
$$\mathcal{D}_y = \mathbf{Z}v$$

with d a uniform random noise of maximum amplitude $\bar{d}$ and v a uniform random noise of maximum amplitude $\bar{v}$. The simulation setup is shown in Fig. 2.

Using the methodology described in Section 4, we compute the observer gain for the system (1) :

$$\mathbf{L} = \begin{pmatrix} 0.2669 \\ 0.3792 \\ 0.1456 \\ 3.9957 \end{pmatrix}, \gamma = 24.1611,$$

$$\mathbf{P} = \begin{pmatrix} 0.7530 & -0.1680 & -0.0530 & -0.0005 \\ -0.1680 & 0.8933 & -0.0896 & -0.0097 \\ -0.0530 & -0.0896 & 2.2650 & -0.0003 \\ -0.0005 & -0.0097 & -0.0003 & 0.0010 \end{pmatrix} 10^5$$

For comparison purposes, a robust state observer was designed using the methodology described in Section 4 but using the state vector $\mathbf{x}$ instead of $\mathbf{x}_e$, thus removing the integral action. The parameters computed for this observer are :

$$\mathbf{L}_r = \begin{pmatrix} 0.0041 \\ 0.0049 \\ 0.0023 \end{pmatrix}, \gamma_r = 0.0352,$$

$$\mathbf{P}_r = \begin{pmatrix} 47.9067 & -41.7438 & -5.7833 \\ -41.7438 & 63.6976 & -7.4568 \\ -5.7833 & -7.4568 & 75.2937 \end{pmatrix}$$

Fig. 3 shows the evolution of the states and output of the real system and the states estimated by the designed robust PI observer and by the same robust observer but without the estimation of d. Three simulations were performed using the same power profile but different disturbance and noise signals. The power profile was generated using piece-wise constant power levels of random magnitude such that the parameter ρ takes values in its full range of variation. The evolution of the varying parameter ρ and of its estimation are shown, the mismatch between them can be explained by the estimation errors on the state and the tendency of ρ to vary abruptly.

Fig. 4 shows the evolution of the estimation error for each state of the system, in each simulation and for both the robust PI observer and the robust observer. It shows that for every scenario, the estimation error of the robust PI observer tends to 0, while the estimation of the robust observer is not. Thus, the proposed observer is robust to piece-wise constant disturbances affecting the system.

Fig. 5 shows that for each simulation the robust PI observer is able to reconstruct the value of d.

Fig. 6 shows the influence of the parameter θ in the quality of the disturbance estimation. Multiple simulations were ran using different observer gains $\mathbf{L}$ based on different values of θ chosen for the design. We can see that higher values for θ allow a faster but noisier convergence of the estimation. Lower values for θ allow a smoother but slower convergence of the estimation. Parameter θ can then be used as a tuning parameter for the observer taking into account the noise levels affecting the state and output of the considered system. In our example $\theta = 0.25$ appeared to be a good trade-off.

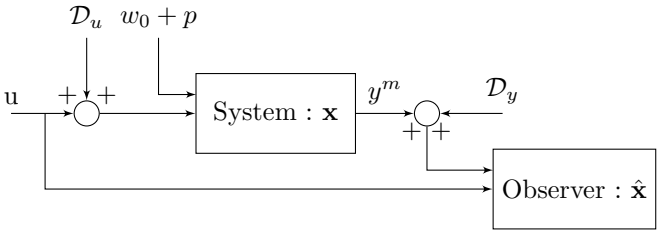

Fig. 2. Simulation setup for design validation. The gas exchange model generates the current state $\mathbf{x}$ and the state observer the state estimation $\hat{\mathbf{x}}$ from input and output measurements. Here, the observer is either the PI robust observer or the robust observer.

In practice, estimated values of gas exchange variables and basal power are used by practitioners to characterize the effort performed. For example, the respiratory quotient (RQ) allows to estimate the contribution of carbohydrates and fats oxidized during the exercise and is defined as follows :

$$RQ = \frac{VCO_2}{VO_2} = \frac{\delta_1 mCO_2}{\delta_2 mO_2} \tag{19}$$

With VCO_2, the volume of CO_2 produced per unit of time, VO_2, the volume of O_2 consumed per unit of time, $\delta_1 = 1.429kg/m^3$, the density of O_2 at $20°C$, $\delta_2 = 1.842kg/m^3$, the density of CO_2 at $20°C$. It is known that values of RQ around 1 suggest that carbohydrates are oxidized and values of RQ around 0.7 suggest that fats are oxidized.

Fig. 7 shows the values of RQ computed for each simulation and their estimated values using the robust PI observer and the robust observer. We can see that the estimation provided by the robust PI observer are accurate and that the estimation of RQ provided by the robust observer can show significant mismatch. For example, in $RQ1$ and $RQ2$, the robust observer fails to recover the real RQ between $t = 500sec$ and $t = 950sec$. This shows that even if the estimation errors are slightly higher with the robust observer for the chosen levels of disturbance p, the consequences in the interpretation of the results can be significant.

6. CONCLUSION

In this paper, we have presented a proportional integral observer design method for estimating the instantaneous basal power during cycling.

Since the physiological model of gas exchange dynamics concerns an uncertain linear parameter varying model, the proposed observer design is based on a robust H_∞ synthesis by solving a family of LMI.

The approach has been tested and validated in simulation for several possible cases of disturbances and possible choices of disturbance model parameters, and compared with respect to a robust observer without disturbance estimation.

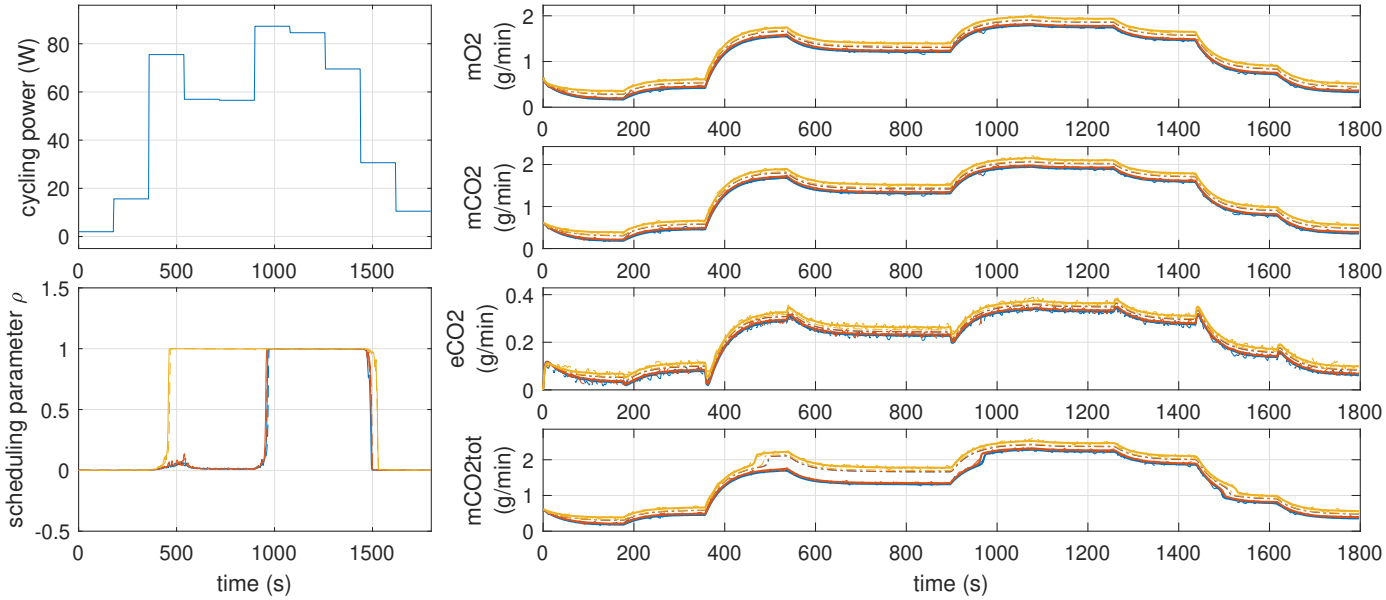

Fig. 3. Evolution of the states and output of the real system, in full lines ——, and of their estimation by the PI observer, in dashed lines - - , and by the robust observer, in dotted lines -·-, to a step input function.

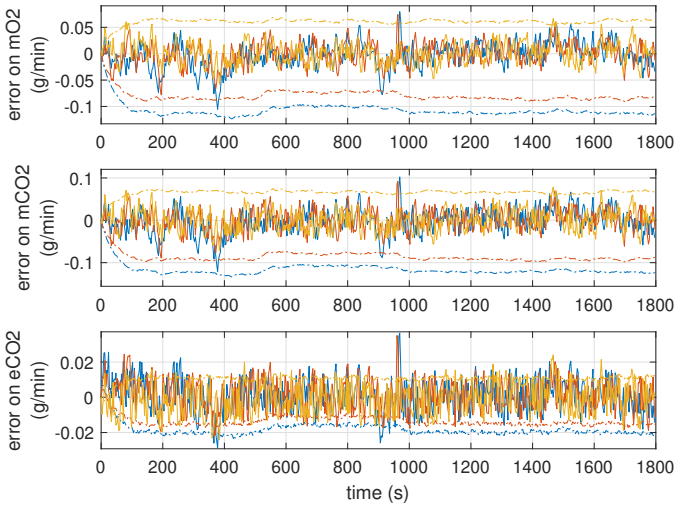

Fig. 4. State estimation errors after simulating 3 times the system for the same power profile but different noises and disturbances affecting the system. The errors of the PI observer are shown in full lines ——, the errors of the robust observer in dotted lines -·-.

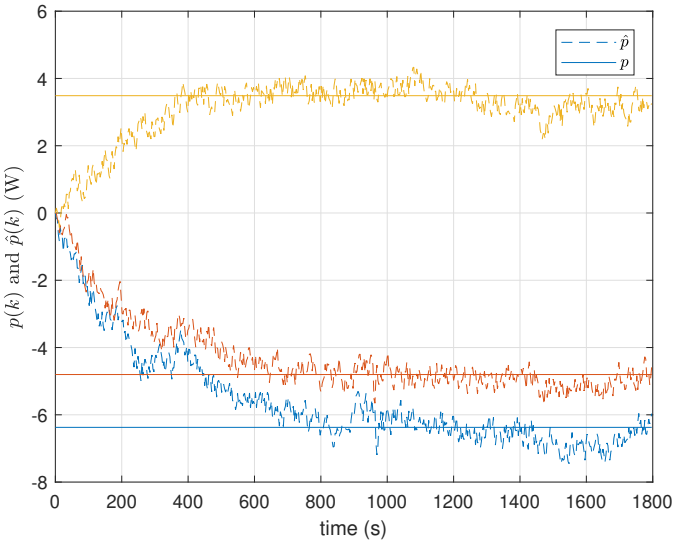

Fig. 5. Estimation of the constant disturbance p after simulating 3 times the system for the same power profile but different noises and disturbances affecting the system.

REFERENCES

Altini, M., Penders, J., and Amft, O. (2016). Estimating Oxygen Uptake During Nonsteady-State Activities and Transitions Using Wearable Sensors. *IEEE Journal of Biomedical and Health Informatics*, 20(2), 469–475. doi:10.1109/JBHI.2015.2390493. URL `http://ieeexplore.ieee.org/document/7006640/`.

Apkarian, P., Gahinet, P., and Becker, G. (1995). Self-scheduled H control of linear parameter-varying systems: a design example. *Automatica*, 31(9), 1251–1261. doi:10.1016/0005-1098(95)00038-X. URL `https://linkinghub.elsevier.com/retrieve/pii/000510989500038X`.

Baig, D.e.Z., Savkin, A.V., and Celler, B.G. (2012). Estimation of oxygen consumption during cycling and rowing. In *2012 Annual International Conference of the IEEE Engineering in Medicine and Biology Society*, 711–714. IEEE, San Diego, CA. doi:10.1109/EMBC.2012.6346030. URL `http://ieeexplore.ieee.org/document/6346030/`.

Beaver, W.L., Wasserman, K., and Whipp, B.J. (1986). A new method for detecting anaerobic threshold by gas exchange. *Journal of Applied Physiology*, 60(6), 2020–2027. doi:10.1152/jappl.1986.60.6.2020. URL `https://www.physiology.org/doi/10.1152/jappl.1986.60.6.2020`.

Beltrame, T., Amelard, R., Wong, A., and Hughson, R.L. (2017). Prediction of oxygen uptake dynamics by machine learning analysis of wearable sensors during activities of daily living. *Scientific Reports*, 7(1), 45738.

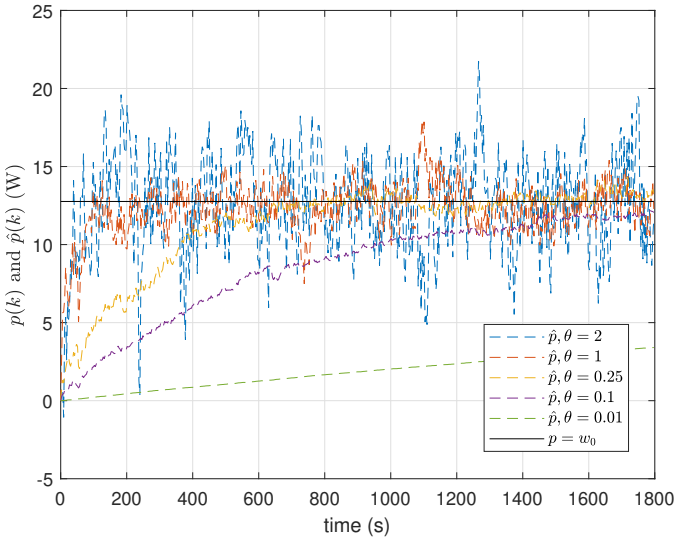

Fig. 6. Estimation of the constant disturbance $p = w_0$ after simulating 5 times the system with different gains for the observer based on a different value for θ in the design process.

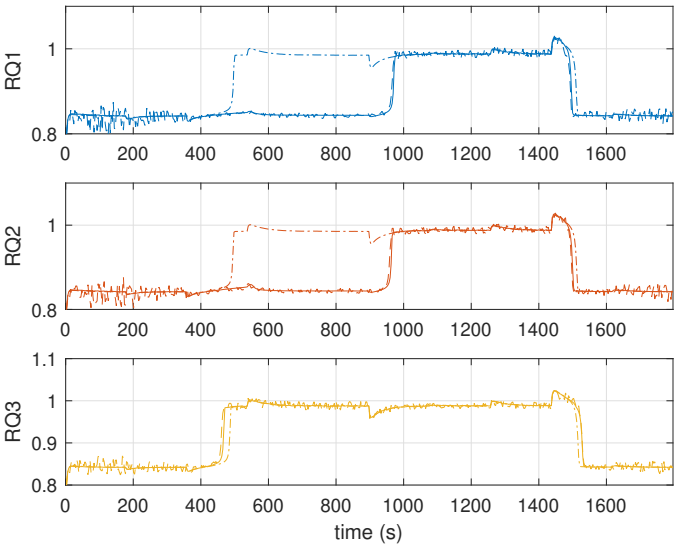

Fig. 7. Respiratory quotient (RQ) for each of the simulations. The RQ of the real system is shown in full lines —, its estimation by the robust PI observer is shown in dashed lines `--` and its estimation by the robust observer is shown in pointed lines `-·-`.

doi:10.1038/srep45738. URL `http://www.nature.com/articles/srep45738`.

Chen, W.H., Yang, J., Guo, L., and Li, S. (2016). Disturbance-observer-based control and related methods—an overview. 63(2), 1083–1095. doi:10.1109/tie.2015.2478397. URL `https://doi.org/10.1109/tie.2015.2478397`.

Gilliat-Wimberly, M., Manore, M.M., Woolf, K., Swan, P.D., and Carroll, S.S. (2001). Effects of habitual physical activity on the resting metabolic rates and body compositions of women aged 35 to 50 years. 101(10), 1181–1188. doi:10.1016/s0002-8223(01)00289-9. URL `https://doi.org/10.1016/s0002-8223(01)00289-9`.

Grant, M. and Boyd, S. (2008). Graph implementations for nonsmooth convex programs. In V. Blondel, S. Boyd, and H. Kimura (eds.), *Recent Advances in Learning and Control*, Lecture Notes in Control and Information Sciences, 95–110. Springer-Verlag Limited. `http://stanford.edu/~boyd/graph_dcp.html`.

Grant, M. and Boyd, S. (2014). CVX: Matlab software for disciplined convex programming, version 2.1. `http://cvxr.com/cvx`.

Grover, R.F. (1963). Basal oxygen uptake of man at high altitude. 18(5), 909–912. doi:10.1152/jappl.1963.18.5.909. URL `https://doi.org/10.1152/jappl.1963.18.5.909`.

Han, J. (2009). From PID to active disturbance rejection control. 56(3), 900–906. doi:10.1109/tie.2008.2011621. URL `https://doi.org/10.1109/tie.2008.2011621`.

Harris, J.A. and Benedict, F.G. (1918). A biometric study of human basal metabolism. 4(12), 370–373. doi:10.1073/pnas.4.12.370. URL `https://doi.org/10.1073/pnas.4.12.370`.

Henry, C. (2005). Basal metabolic rate studies in humans: measurement and development of new equations. 8(7a), 1133–1152. doi:10.1079/phn2005801. URL `https://doi.org/10.1079/phn2005801`.

Johnson, C. (1968). Optimal control of the linear regulator with constant disturbances. 13(4), 416–421. doi:10.1109/tac.1968.1098947. URL `https://doi.org/10.1109/tac.1968.1098947`.

Johnson, C.D. (2008). Real-time disturbance-observers origin and evolution of the idea part 1: The early years. IEEE. doi:10.1109/ssst.2008.4480196. URL `https://doi.org/10.1109/ssst.2008.4480196`.

Martinez, J.J., Loukkas, N., and Meslem, N. (2018). H-infinity set-membership observer design for discrete-time LPV systems. *International Journal of Control*, 1–12. doi:10.1080/00207179.2018.1554910. URL `https://www.tandfonline.com/doi/full/10.1080/00207179.2018.1554910`.

McConnell, W.J. (1925). BASAL METABOLISM AS AFFECTED BY ATMOSPHERIC CONDITIONS. 36(3), 382. doi:10.1001/archinte.1925.00120150091005. URL `https://doi.org/10.1001/archinte.1925.00120150091005`.

McMurray, R.G., Soares, J., Caspersen, C.J., and McCurdy, T. (2014). Examining variations of resting metabolic rate of adults. 46(7), 1352–1358. doi:10.1249/mss.0000000000000232. URL `https://doi.org/10.1249/mss.0000000000000232`.

Melzer, K., Heydenreich, J., Schutz, Y., Renaud, A., Kayser, B., and Mäder, U. (2016). Metabolic equivalent in adolescents, active adults and pregnant women. 8(7), 438. doi:10.3390/nu8070438. URL `https://doi.org/10.3390/nu8070438`.

Ohishi, K., Nakao, M., Ohnishi, K., and Miyachi, K. (1987). Microprocessor-controlled DC motor for load-insensitive position servo system. IE-34(1), 44–49. doi:10.1109/tie.1987.350923. URL `https://doi.org/10.1109/tie.1987.350923`.

Rosero, N., Martinez, J.J., and Corno, M. (2018). Modeling of gas exchange dynamics using cycle-ergometer tests. *IFAC-PapersOnLine*, 51(2), 349–354. doi:10.1016/j.ifacol.2018.03.060. URL `https://linkinghub.elsevier.com/retrieve/pii/S2405896318300648`.

Sariyildiz, E., Oboe, R., and Ohnishi, K. (2020). Disturbance observer-based robust control and its applications: 35th anniversary overview. 67(3), 2042–2053. doi:10.1109/tie.2019.2903752. URL https://doi.org/10.1109/tie.2019.2903752.

Shandhi, M.M.H., Bartlett, W.H., Heller, J., Etemadi, M., Young, A., Ploetz, T., and Inan, O. (2020). Estimation of Instantaneous Oxygen Uptake during Exercise and Daily Activities using a Wearable Cardio-Electromechanical and Environmental Sensor. *IEEE Journal of Biomedical and Health Informatics*, 1–1. doi:10.1109/JBHI.2020.3009903. URL https://ieeexplore.ieee.org/document/9143414/.

She, J.H., Fang, M., Ohyama, Y., Hashimoto, H., and Wu, M. (2008). Improving disturbance-rejection performance based on an equivalent-input-disturbance approach. 55(1), 380–389. doi:10.1109/tie.2007.905976. URL https://doi.org/10.1109/tie.2007.905976.

She, J.H., Xin, X., and Pan, Y. (2011). Equivalent-input-disturbance approach—analysis and application to disturbance rejection in dual-stage feed drive control system. 16(2), 330–340. doi:10.1109/tmech.2010.2043258. URL https://doi.org/10.1109/tmech.2010.2043258.

Spurway, N.C. (1992). Aerobic exercise, anaerobic exercise and the lactate threshold. *British Medical Bulletin*, 48(3), 569–591. doi:10.1093/oxfordjournals.bmb.a072564. URL https://academic.oup.com/bmb/article/297779/Aerobic.

Su, S.W., Wang, L., Celler, B.G., and Savkin, A.V. (2007). Oxygen Uptake Estimation in Humans During Exercise Using a Hammerstein Model. *Annals of Biomedical Engineering*, 35(11), 1898–1906. doi:10.1007/s10439-007-9362-2. URL http://link.springer.com/10.1007/s10439-007-9362-2.

Wasserman, K. (1984). The Anaerobic Threshold Measurement to Evaluate Exercise Performance [1, 2]. *American Review of Respiratory Disease*, 129(2P2), S35–S40. doi:10.1164/arrd.1984.129.2P2.S35. URL http://www.atsjournals.org/doi/10.1164/arrd.1984.129.2P2.S35.